Determination of the Porosity of Granular Soils Using Electrical Resistivity Measurements

Zaid Al-Qaysi

UNDERGRADUATE STUDENT, DEPARTMENT OF CIVIL AND ENVIRONMENTAL ENGINEERING
WESTERN UNIVERSITY, LONDON, ONTARIO, CANADA. EMAIL: ZALQAYSI@UWO.CA

Abouzar Sadrekarimi, Ph.D., P. Eng.

DEPARTMENT OF CIVIL AND ENVIRONMENTAL ENGINEERING
WESTERN UNIVERSITY, LONDON, ONTARIO, CANADA

ABSTRACT

The difficulty of sampling saturated cohesionless soils for assessing their in-situ porosity (void ratio) due sample disturbance and the expensive methods of obtaining undisturbed field samples has increased the need for finding inexpensive methods for estimating the in-situ porosity. The approach of using geophysical techniques by measuring the electrical resistance of cohesionless soil can be used to define many geotechnical parameters and physical properties of sand without the need to obtain field samples, thereby minimizing the effects of soil disturbance. This paper presents an experimental testing program for investigating the effects of pore water salinity, soil fabric, void ratio, and fines content on electrical resistivity of saturated sands. The results show that the electrical resistivity of saturated sands decreases with increasing void ratio, increasing electrolyte concentration, and decreasing fines content at a certain void ratio, while sand fabric and gradation have relatively minor influences. Empirical correlations are thus developed for estimating sand porosity and hydraulic conductivity. The proposed correlations can be useful engineering tools to determine the in-situ void ratio and seepage characteristics of sands.

Introduction

The behavior of cohesionless soils is largely controlled by their density and porosity. For example, Figure 1 illustrates the effect of porosity on the undrained shearing behavior of saturated Illinois river sand specimens in triaxial compression shear tests (Sadrekarimi, 2009). Therefore, determination of in-situ porosity and thus density of sands is essential for replicating the in-situ shearing behavior and predicting field strength and liquefaction susceptibility behavior, densification control, as well as determining seepage characteristics of cohesionless soils. These parameters at the top 10 m of a seabed are particularly important for the design of most offshore structures (e.g. oil platforms, wind turbine foundations, oil pipelines).

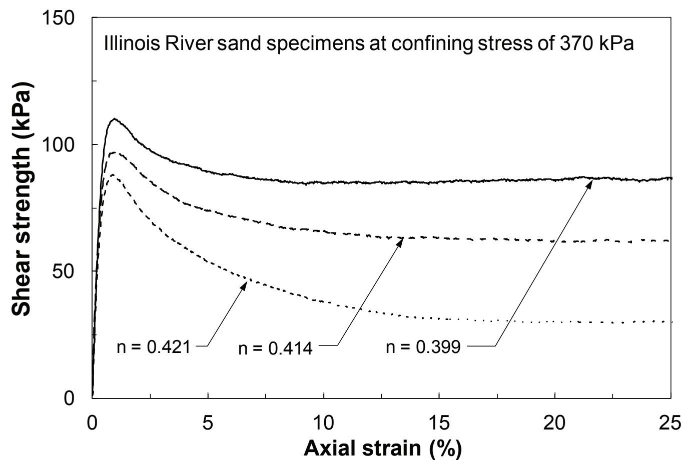

Figure 1: Effect of porosity (*n*) on the undrained shearing behavior of Illinois river sand in triaxial compression tests (Sadrekarimi, 2009)

However, direct measurement of the in-situ porosity and density of cohesionless soils is challenging due to the difficulties in obtaining undisturbed samples for laboratory testing and the susceptibility of cohesionless soil samples to disturbance caused by borehole excavation, sampling, during transportation, and sample extrusion and handling. In particular, saturated sands are notoriously difficult to sample without disturbance. Even carefully collected, thin-wall cores are likely to collapse during sampling or sample extrusion resulting in an underestimation of the in-situ porosity. This becomes further complicated by the inherent variability of field soil deposits which makes even the few high-quality undisturbed samples inadequate for characterizing subsurface soil conditions. These challenges have increased the need of finding more reliable and cost-effective in-situ testing methods. Geophysical techniques, including soil electrical resistivity measurement, can be used to define many geotechnical parameters and physical properties of sand without obtaining field samples, and thus minimize soil disturbance effects. The objective of this study is to establish a relationship between electrical resistivity, hydraulic conductivity, and porosity of granular soils.

Theoretical Basis

Electrical resistivity, ρ (Ohm·m) of a material is a measure of how well the material retards the flow of an electrical current. As particles (composed of quartz, feldspar, or carbonates) of a cohesionless soil are often non-conductive and act as insulators, the flow of an electrical current through a saturated granular soil occurs primarily through the pore water. Therefore, conductivity, volume, and the distribution of the pore water control the bulk electrical resistivity of sands (ρ_b). Accordingly, ρ_b can be directly related to the pore water resistivity (ρ_f) and pore volume (characterized by soil porosity n) using the following general empirical relationship (Archie, 1942; Daniel et al., 2003; Winsauer et al., 1952):

$$\frac{\rho_b}{\rho_f} = an^{-m} \qquad (1)$$

Where exponent m and coefficient a are fitting parameters which depend on pore volume tortuosity and soil particle cementation. These parameters can be determined from laboratory calibration experiments. The ratio ρ_b/ρ_f is known as the "formation factor" (*FF*) which is employed to remove the effects of changes in pore water resistivity (as sand particles are insulators) and geometrical characteristics of the measuring probe from the electrical resistivity of a saturated sand. Similar to ρ_b, *FF* is an intrinsic property of a soil which depends on the volume and the geometry of soil pore spaces.

Experimental Program

The experiments of this study were aimed to determine the effects of fines content, sand fabric, salt concentration and void ratio on the electrical resistivity of sands as discussed in the following paragraphs.

Sample preparation

Sand samples were prepared using undercompaction moist tamping in a cylindrical acrylic chamber with an internal diameter and height of 114.4 mm and 250 mm, respectively. The samples were then saturated by inundating them with water. In the moist tamping method, the dry sand was premixed with 5% moisture and thoroughly mixed to uniformly distribute the moisture content. Then predetermined weights of the moist sand were deposited and tamped in 5 layers of 50 mm thick using an adjustable-height handheld tamper. Moist tamping replicates conditions where moist sand is dumped as a fill and subsequently submerged as the water table rises (Chu and Leong, 2003; Olson et al., 2000). The weight of wet soil placed in the lower layers was intentionally less than those of the upper layers in order to account for the increase in soil density as a result of tamping the successive overlying layers and improve specimen uniformity. The difference in density between successive layers is defined as the undercompaction ratio (Ladd, 1978). Based on an undercompaction ratio of 10%, the density of each layer was increased linearly from the bottom to the top of the specimen. This method led to more uniform samples and repeatable test results.

Materials

Two gradations of Ottawa sand (called "Barco 32" and "Barco 71") as well as a local silty sand (with a fines content of 11%) from the Boler Mountain (London, Ontario) were used in the experiments of this investigation. The particles of Barco 32 and Barco 71 sands are purely quartz with rounded to subrounded shapes, while the Boler Mountain sand is composed of subrounded to subangular particle shapes with mixed mineralogy of quartz, feldspar and carbonates. Barco 71 sand was mixed with different amounts of quartz silt particles to produce different silty sands and investigate the effect of fines content (FC). Figure 2 shows the gradations of these materials and Table 1 presents their physical properties. The specific gravity of sand particles (G_s), and maximum (e_{max}) and minimum (e_{min}) void ratios of the sands were obtained following the ASTM standard procedures (ASTM, 2006a, b, c).

Sand	G_s	e_{min}	e_{max}
Barco 32	2.65	0.530	0.798
Barco 71	2.65	0.498	0.821
Boler Mountain	2.65	0.450	0.945

Table 1. Physical properties and index characteristics of the tested sands

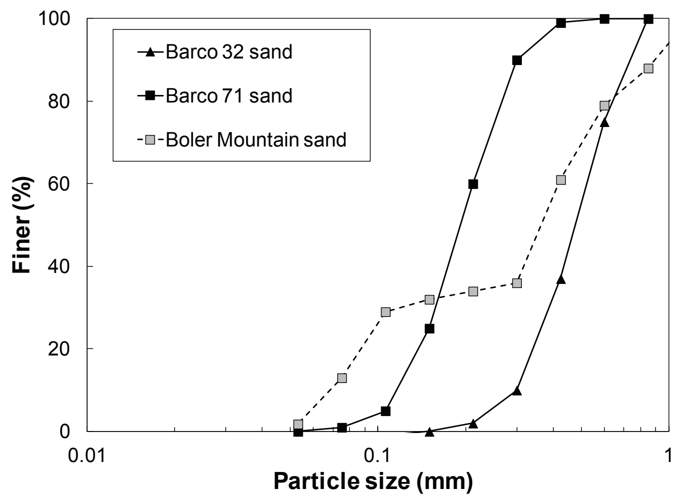

Figure 2: Particle size distributions of the sands used in this study

Electrical resistivity measurement

A portable electrical resistivity probe (Stevens Water Monitoring System Inc, 2007) was used to measure the electrical resistance (*R*) as well as the temperature of the soil water system. This probe introduces an electrical current (*I*) into the soil sample at a certain depth through four electrodes, and measures the potential voltage difference (*V*) between them. The average electrical resistance of the soil sample around the electrodes is then calculated from Ohm's law ($R = V/I$). These data are transferred to and displayed on a handheld PDA. Soil electrical resistivity (ρ_b), a fundamental soil property, is obtained by multiplying the measured resistance (*R*) by the geometrical factor, *K* of the probe ($\rho_b = K \times R$) which depends on the size and the separation of the electrodes. An average geometrical factor of 0.872 was determined for the probe by calibration in an ionic buffer solution of 3gr/L salt (NaCl) with a known resistivity of 0.052 Ohm.m. All experiments were performed at a controlled laboratory temperature of 20°C and in a non-metallic (acrylic) cylinder as metal could interfere with the measurements.

Results and Discussion

The results of the experiments are presented below. For each experiment, sample void ratio and porosity was determined based on the weight of the soil used for sample preparation and sample volume while ρ_b was measured using the electrical resistivity probe.

Effect of electrolyte concentration

Electrical resistivity of the pore water (ρ_f) depends on the electrolyte concentration as a result of pore water salinity, and thus at a certain void ratio the electrical resistance of a saturated cohesionless soil would become a function of the amount of salt in the pore fluid. Figure 3 presents the electrical resistance of saturated Barco 71 sand samples with different amounts of pore water salinity expressed in grams of salt per 1 liter of distilled water. Based on this figure, salt content of the pore fluid electrolyte has a profound impact on the electrical resistance of soil as R decreases with increasing salt concentration of the pore water.

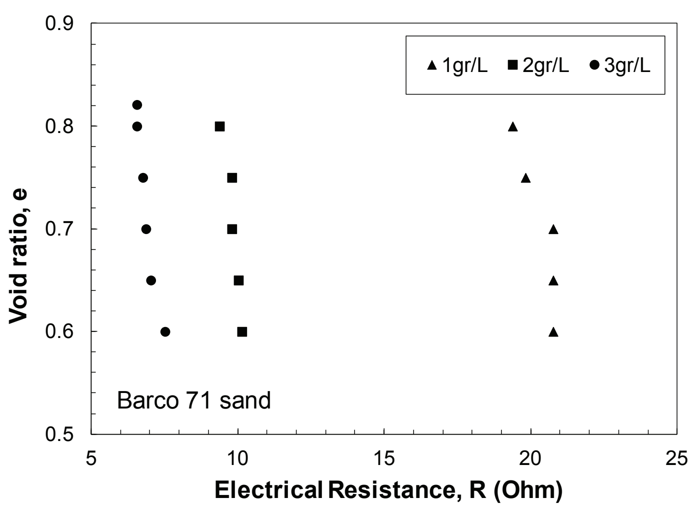

Figure 3: Effect of pore water salinity on electrical resistance of saturated Barco 71 sand samples

Figure 3 further indicates that soil electrical resistance is inversely related to its void ratio. As void ratio increases, the electrical resistance decreases and the electrical conductivity increases. Increasing of the electrical conductivity is due to the increase of the conducting pore water volume among the sand particles and the ability of the electrolyte water to conduct electricity, reducing the electrical resistivity of the saturated sand.

Effect of particle size distribution

Figure 4 compares the electrical resistances of the different sands tested in this study, which clearly indicates increasing soil electrical resistance with increasing of the amount of fines. Increasing fines content, even at the same void ratio, reduces the number and the volume of connections among the pores of a sand and thus the electrical connectivity and conductivity of the pore fluid. Despite differences in particle size distributions (see Fig. 2), the Barco 32 and Barco 71 sands exhibit nearly similar electrical resistance at FC = 0%, or the Boler Mountain and Barco 71 sands with about 10% fines contents show similar electrical resistances. Hence, the effect of variations in particle size distribution on the electrical resistance of sands seems to be secondary to the effect of FC. A similar observation was made by Keller and Frischkecht (1966).

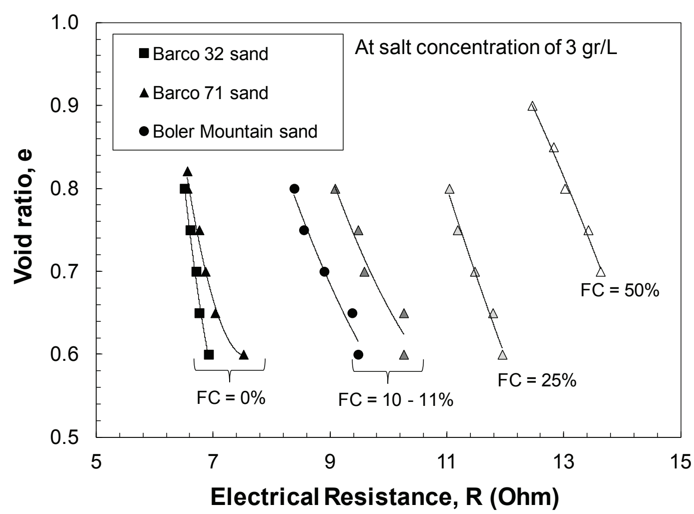

Figure 4: Effect of sand particle size distribution and fines content (FC) on electrical resistance with a pore water salt concentration of 3 gr/L

Effect of specimen preparation method

In order to investigate the effect of sand fabric on the electrical resistivity of saturated sands, a number of experiments were conducted on samples prepared by air and water pluviation methods. These methods resemble sand fabrics formed by natural aeolian and fluvial process (e.g. in rivers and streams), respectively (Oda et al., 1978; Vaid and Eliadorani, 1998). Air pluviated specimens were prepared by raining sand particles into the cylindrical mold through air. The void ratio and density of the samples prepared by air pluviation was varied by changing the free-fall height and thus the depositional velocity of the particles. For preparing very loose samples, sand particles were rained with nearly zero drop height. A similar procedure was used to prepare water pluviated specimens by raining sand particles through water. However, as the particles reach a terminal velocity after a certain drop height in water, different void ratios were produced by tamping the sides of the specimen mold and thus densifying the sand sample. Figure 5 shows the results of these experiments. Electrical resistances of the samples prepared by the pluviation methods fall nearly on the same trendline, despite the larger void ratios of the water pluviated samples. However, the electrical resistances of the moist tamped samples are slightly greater which is likely because of the comparatively isolated pores of the honeycomb moist tamped sand fabric.

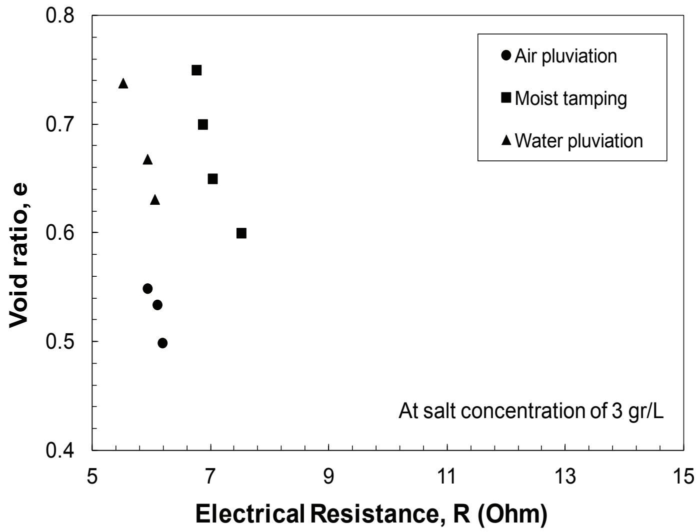

Figure 5: Effect of specimen preparation method on electrical resistance of sand

Estimation of porosity

In order to develop a practical relationship, the effects of electrolyte salinity and probe geometry are removed by presenting the results in terms of formation factor (*FF*) and porosity (*n*) in Figure 6. Electrical resistivity data for several other sands (platy sand, sand with 1% shell content, rounded sand, and sand and gravel) with different particle size distributions and particle shapes (Arulmoli et al., 1985; Jackson et al., 1978) are also included in this figure. According to Figure 6, *FF* generally increases with decreasing sand porosity (or increasing density) due to the smaller water saturated pore volume of dense sands. According to these data, variations in gradation, mean particle size, and particle shape have little influence on the trend of data. The most significant changes in *FF* are produced by changes in FC, while the scatter at certain FC could be because of variations in sand gradation and method of sample preparation.

Data at certain FC are also curve fitted with Equation [1] and the fitting parameters (*a*, *m*) are shown in Figure 6. In contrast to other studies, rather than particle shape (Jackson et al., 1978) or cementation (Archie, 1942), Figure 6 indicates that the parameters of Equation [1] largely depend on FC. Coefficient *a* and the exponent *m* respectively increase and decrease with increasing FC. Fine particles increase the tortuosity and thus the length of the path that an electrical current must follow as well as constricting the openness of these flow channels. And therefore *FF* increases with increasing FC. As the experiments of this study were performed at small stress levels (< 5 kPa) the effect of stress level cannot be inferred from these results. However, based on past experimental observations (Hulbert et al., 1982; Lee et al., 2008), *FF* varies with stress to the extent that soil porosity is altered by stress. In other words, at a certain porosity stress does not appear to affect *FF*.

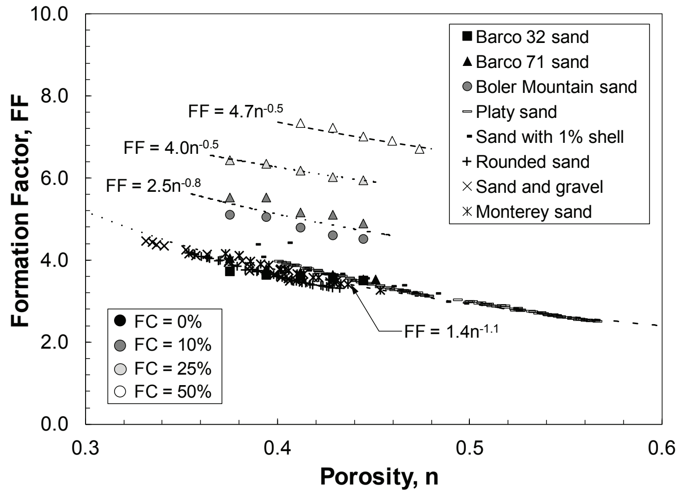

Figure 6: Effect of porosity on *FF* for the cohesionless soils tested in this study as well as for several other sands (Arulmoli et al., 1985; Jackson et al., 1978)

Estimation of Hydraulic Conductivity

Besides electrical resistivity, constant head permeability tests were carried out to measure the hydraulic conductivity (*k*) of similar samples. Figure 7 shows unique relationships (similar to Eq. [1]) between the results of these experiments with *FF* as well as those from Jones and Buford (1951) at certain FC. These data show that for a cohesionless soil with a certain fines content, a lower *FF* would indicate an aquifer with higher hydraulic conductivity and yield. The good relationship between *FF* and hydraulic conductivity is somewhat expected as both electrical current and fluid flow move in tortuous paths through the intergranular pores of a soil. Particularly in sandy soils where there is no interaction between the ionic constituents of the porewater and the matrix solid, the bulk resistivity of a soil-water system would be a function of pore volume tortuosity, and porosity and hence hydraulic conductivity.

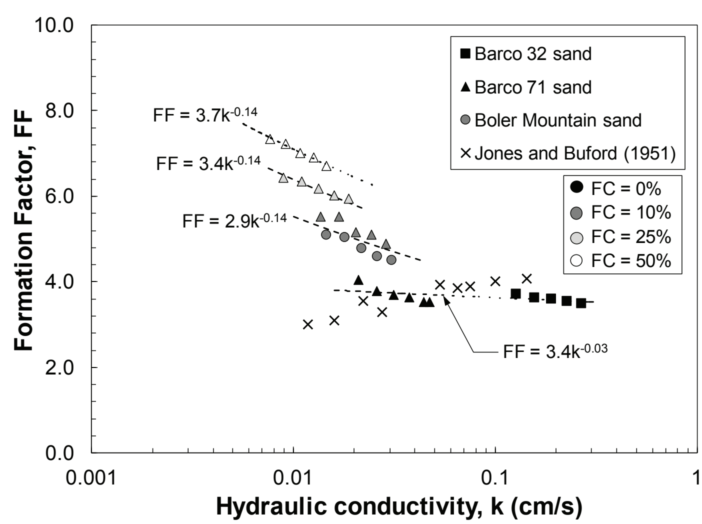

Figure 7: Variations of hydraulic conductivity and *FF* for the cohesionless soils of this study as well as for a sand from Jones and Buford (1951)

Note that the plots of Figures 6 and 7 as well as the findings of this paper are only applicable to saturated cohesionless soils with non-conductive particles. The result might be inapplicable for clayey, organic, or cemented soils as the surface conduction of clay particles could dominate the electrical resistivity of a clayey soil (Erickson and Jarrard, 1998).

Field Applications

Site specific calibration is always recommended for using electrical resistivity measurements for estimating sand porosity, yet in the absence of such data the correlations presented in Figures 6 and 7 can be employed to determine the in-situ density and seepage characteristics of sands. This method can be applied to the electrical resistivity measurements of a resistivity cone penetrometer (RCPTu) to identify soil stratigraphy as well as soil porosity and hydraulic conductivity. This will provide an additional level of redundancy to the existing empirical methods of estimating the void ratio (i.e. porosity) of cohesionless soils from CPTu. In addition to RCPTu, electrical resistivity tomography could be used for obtaining three dimensional resistivity images of the subsurface and thus a more extensive characterization of soil porosity. In particular, an initial surface electrical resistivity surveying prior to drilling and sampling would help to locate loose and potentially liquefiable cohesionless soils and assist in selecting strategic borehole locations and sampling prior to drilling. Therefore, an integrated geophysical, geologic, and drilling study would provide a more rapid, cost effective, and accurate understanding of the subsurface.

Since changes in electrical resistivity result from changes in pore water volume, the application of this method would require saturated soil conditions. Offshore and seabed sediments would thus be the ideal conditions for the application of this method as they are naturally saturated with ionized sea water. In particular, the in-situ resistivity of pore water (ρ_f) – which is needed to calculate *FF* – can be readily measured just before the probe penetrates into the sediment without taking water samples. Although some other techniques like the nuclear magnetic resonance method, gamma-ray absorption techniques or X-ray tomography may allow higher resolution porosity determination, these methods involve highly complex and expensive instrumentation. Whereas electrical resistivity measurement and interpretation is fast, reliable, and low-cost.

Conclusions

The results of this study show that the electrical resistivity of cohesionless soils decreases with increasing pore water salinity, and porosity while soil fabric, particle size distribution and shape of the particles have negligible effects on electrical resistivity for clean sands. However, the amount of fine particles (< 0.075 mm) has a profound impact on the resistivity of a saturated cohesionless soil to an electrical current. Accordingly, a number of correlations are developed between electrical resistivity, and porosity and hydraulic conductivity of cohesionless soils for certain fines contents. Measurement of void ratio and in-situ density of cohesionless soils could be difficult due to sample disturbance and the inherent variability of in-situ soils.

References

Archie, G.E., 1942. The electrical resistivity log as an aid in determining some reservoir characteristics. Transactions of the American Institute of Mining and Metallurgical Engineers Petroleum Division 146, 54 – 62.

Arulmoli, K., Arulanandan, K., Seed, H.B., 1985. New method for evaluating liquefaction potential. Journal of Geotechnical Engineering 111, 95-114.

ASTM, 2006a. Standard D854: Standard Test Methods for Specific Gravity of Soil Solids by Water Pycnometer, Annual Book of ASTM Standards. ASTM International, West Conshohocken, PA, pp. 100 – 106.

ASTM, 2006b. Standard D4253: Standard test methods for maximum index density and unit weight of soils using a vibratory table., Annual Book of ASTM Standards. ASTM International, West Conshohocken, PA.

ASTM, 2006c. Standard D4254: Standard test methods for minimum index density and unit weight of soils and calculation of relative density., Annual Book of ASTM Standards. ASTM International, West Conshohocken, PA.

Chu, J., Leong, W.K., 2003. Reply to the discussion by A. Eliadorani and Y.P. Vaid on "Effect of undrained creep on instability behaviour of loose sand". Canadian Geotechnical Journal 40, 1058-1059.

Daniel, C.R., Campanella, R.G., Howie, J.A., Giacheti, H.L., 2003. Specific depth cone resistivity measurements to determine soil engineering properties. Journal of Environmental and Engineering Geophysics 8, 15 – 22.

Erickson, S.N., Jarrard, R.D., 1998. Porosity/formation-factor relationships for siliciclastic sediments from Amazon Fan. Geophysical Research Letters 25, 2309 – 2312.

Hulbert, M.H., Bennett, R.H., Lambert, D.N., 1982. Seabed geotechnical parameters from electrical conductivity measurements. Geo-Marine Letters 2, 219 – 222.

Jackson, P.D., Taylor-Smith, D., Stanford, P.N., 1978. Resistivityporosity-shape relationships for marine sands. Geophysics 43, 1250 – 1268.

Jones, P.H., Buford, T.B., 1951. Electric logging applied to ground-water exploration. Geophysics 16, 115 – 139.

Keller, G.V., and Frischknecht, F. C. , 1966. Electrical methods in geophysical prospecting. Pergamon Press, New York.

Ladd, R.S., 1978. Preparing test specimens using undercompaction. Geotechnical Testing Journal, ASTM 1, 16 – 23.

Lee, C., Lee, J.S., Lee, W., Cho, T.H., 2008. Experiment setup for shear wave and electrical resistance measurements in an oedometer. Geotechnical Testing Journal, ASTM 31, 149 – 156.

Oda, M., Koishikawa, I., Higuchi, T., 1978. Experimental study of anisotropic shear strength of sand by plane strain test. Soils and Foundation 18, 25-38.

Olson, S.M., Stark, T.D., Walton, W.H., Castro, G., 2000. 1907 static liquefaction flow failure of the North Dike of Wachusett Dam. J Geotech Geoenviron 126, 1184-1193.

Sadrekarimi, A., 2009. Development of a new ring shear apparatus for investigating the critical state of sands, Department of Civil and Environmental Engineering. University of Illinois, Urbana-Champaign, Urbana, Illinois.

Stevens Water Monitoring System Inc, 2007. Comprehensive Stevens Hydra Probe Users Manual, in: Inc., S.W.M.S. (Ed.). Stevens® Water Monitoring System, Inc., Portland, OR.

Vaid, Y.P., Eliadorani, A., 1998. Instability and liquefaction of granular soils under undrained and partially drained states. Canadian Geotechnical Journal 35, 1053-1062.

Winsauer, W.O., Shearin, H.M., Masson, P.H., Williams, M., 1952. Resistivity of brinesaturated sands in relation to pore geometry. Bulletin of the American American Association of Petroleum Geologists 36, 253 – 257.